20th Australasian Fluid Mechanics Conference
Perth, Australia
5-8 December 2016

Numerical study on the performance of a flapping foil power generator with a passively flapping flat plate

Z. Liu[1], J. C.S. Lai[1], J. Young[1] and F.-B. Tian[1]

[1]School of Engineering and Information Technology
The University of New South Wales, Canberra, Australian Capital Territory 2600, Australia

Abstract

In this study, the flow characteristics of a flapping foil power generator with a passively flapping flat plate have been investigated using the lattice Boltzmann method (LBM) and immersed boundary method at Reynolds number of 1100 based on the chord length. The aim is to explore potential benefits of flow induced passive actuation of the flat plate tail to the power output and efficiency. The problem consists of a rigid NACA0015 foil undergoing prescribed pitch and plunge motions and a tail hinged to the rigid foil using a torsion spring. In this study, kinematic parameters of the flapping foil power generator including pitch and plunge amplitudes, reduced frequency, phase angle between the plunge and pitch motions and pivot location were chosen to be the optimal values of the rigid case suggested by the previous literature and the contours of efficiency computed by the LBM. Apart from the rigid tail case, different tail flexibilities, represented by the frequency ratio of the natural frequency of the structure to the flapping frequency, were considered. Three cases including the rigid tail are explored in detail through histories of lift force, moment and power coefficients and contours of pressure and vorticity. The performance of the flapping foil power generator with a very flexible tail (natural frequency $<$ flapping frequency) degrades due to poor synchronization between aerodynamic loads and prescribed motions. However, an appropriate frequency ratio can enhance the average power coefficient and efficiency. The study provides illustrates about how the passive actuation of the tail affects the formation and transition of the trailing edge vortex and enhances the lift force near stroke reversal.

Introduction

With the increasing demand for renewable energy, power generators harvesting energy from the motion of flapping foils as an alternative to rotary wind and tidal turbines have been under active investigations in the last 10 years. This concept can be traced to McKinney and DeLaurier's test of a 90W flapping foil device and develops rapidly based on increasing number of numerical and experimental studies [11]. In the meantime, several full-scale prototype including Stingray, bioSTREAM and Pulse Hydrofoil were tested[10]. These prior works have focused primarily on activation mode (prescribed, semi-passive and fully passive) and kinematics (e.g. reduced frequency, pitch and plunge amplitudes, phase difference between pitch and plunge) with different foil profiles [10, 11]. According to studies on micro air vehicles using flapping foils to produce thrust inspired by locomotion of insects and fishes, structural flexibility can contribute to high propulsion efficiency [5]. Considering the similarity of flapping foils in thrust and power generation applications, it is speculated that an appropriate coupling between foil deformation and aerodynamic loads acting on the foil may improve the performance of a flapping foil power generator.

In contrast to numerous studies on foil flexibility for performance enhancement in thrust generation, there are only a few studies on the effects of actively and passively flexible foil on the performance of flapping foil power generators [1, 3, 4, 7, 9]. Results for an actively flexible foil show that the formation time of the leading edge vortex (LEV) is a key factor in power generation but power required to deform the foil makes a significant contribution to the overall efficiency of a flapping power generator which is generally neglected in the performance analysis[1, 3, 4]. Studies on passively flexible foils show that a flexible plate as well as a plate with a flexible leading segment and a rigid trailing segment cannot enhance the efficiency[7], while a passively flexible tail is beneficial to the efficiency improvement at relatively low effective angles of attack of 10° and 20°[9] compared to the optimal value of 35°[2].

In this study, a flapping foil power generator with a flexible tail hinged to the foil operating in an uniform flow is simulated. The kinematic parameters chosen are the optimal values for a flapping rigid foil to ensure that any enhancement in efficiency can be attributed to the flexibility alone. The optimal values of the kinematic parameters of a flapping rigid foil are obtained from a previous parametric study[2] and interpolation of the contours of efficiency computed by the lattice Boltzmann method (LBM). The effect of the passive flexibility (in terms of the ratio of the natural frequency of the tail to the flapping frequency) on power-extraction efficiency is discussed.

Physical Problem and Mathematical Formulation

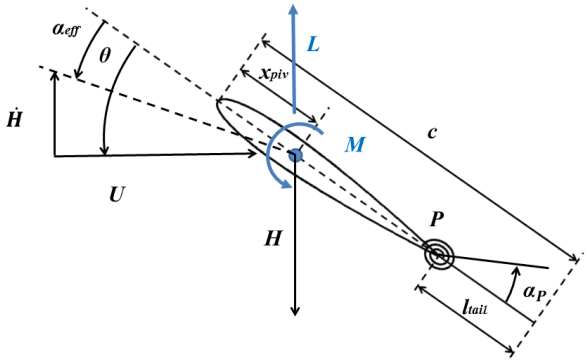

Figure 1: Aerodynamic loads on the foil

A simple two-dimensional model with a NACA0015 foil and a flat plate hinged to the foil using a torsion spring is used for the flexibility study. This torsional-flexibility model converges to the non-linear Euler-Bernoulli beam with the increase of the number of linked flat plates[8]. The rigid foil undergoes prescribed pitch and plunge motions in a uniform flow with veloc-

ity U:

$$\theta(t) = \theta_0 \sin(2\pi f t) \tag{1}$$
$$H(t) = H_0 \sin(2\pi f t + \varphi) \tag{2}$$

where $\theta(t)$ and $H(t)$ are the instantaneous angular and plunge positions respectively; φ is the phase angle between the pitch and plunge motion; x_{piv} is the non-dimensional distance from the leading edge to the pivot point.

The motion of the tail with flexibility modelled by a torsion spring at point P (figure 1) is passively determined by the fluid structure interaction and governed by

$$\begin{aligned} J\ddot{\alpha}_p + k_s\alpha_p =& M_f - \frac{ml_{tail}}{2}\cos(\theta+\alpha_p)\,\ddot{y}_p \\ &+ \frac{ml_{tail}}{2}\sin(\theta+\alpha_p)\,\ddot{x}_p - J\ddot{\theta} \end{aligned} \tag{3}$$

where J and M_f are the moment inertia of the tail and the fluid moment with respect to the point P, respectively; k_s is the spring stiffness; $m = \rho_{tail} l_{tail}$ is the mass of the tail (ρ_{tail} and l_{tail} are the linear density and the length of the tail respectively); $\ddot{y}_p$ and $\ddot{x}_p$ are the vertical and horizontal accelerations of the point P; and α_p and $\ddot{\alpha}_p$ are the angular position and acceleration determined by the fluid and structure interaction.

The performance of a flapping foil power generator is quantified by two non-dimensional parameters, the mean power coefficient $\bar{C}_P$ and efficiency η:

$$\bar{C}_P = \frac{1}{T}\int_{t_0}^{t_0+T} C_P(t)\,dt \tag{4}$$
$$\eta = \bar{C}_P \frac{c}{d} \tag{5}$$

where T is the period; c is the chord length between the leading edge of the NACA foil and the end of the flat plate (figure 1); d is the maximum distance swept by the foil; and $C_P(t)$ is the instantaneous power coefficient expressed as

$$C_P(t) = \frac{P_h(t) + P_\theta(t)}{\frac{1}{2}\rho U^3 c} \tag{6}$$

where ρ is the freestream density; $P_h(t) = L\dot{H}(t)$ is the instantaneous power component due to plunge motion and $P_\theta(t) = M\dot{\theta}(t)$ is the instantaneous power component due to pitch motion; L and M are the lift and moment respectively.

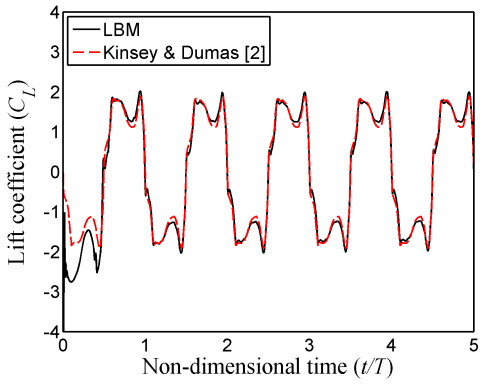

Figure 2: Comparison of lift coefficient with Kinsey and Dumas[2]

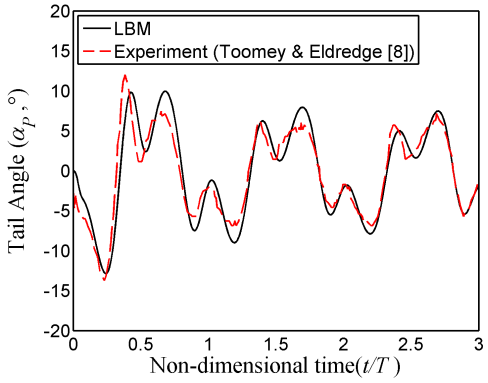

Figure 3: Comparison of the tail angle with Toomey and Eldredge [8]

The incompressible flow is solved by the lattice Boltzmann method (LBM) [6] using a multi-block technique to balance the accuracy and time cost. An immersed boundary method [6] is used to distribute the boundary force to the Cartesian mesh in the vicinity of the solid boundary.

Validations

To validate the fluid solver in predicting energy harvesting performance, results of a flapping NACA0015 foil($f^* = fc/U = 0.14$, $h_0 = H_0/c = 1$, $\theta_0 = 76.3°$, $\varphi = 90°$ and $x_{piv} = 0.333$) are compared with Kinsey and Dumas's work[2]. Figure 2 shows that the instantaneous lift coefficient $C_L = L/(1/2\rho U^2 c)$ is in good agreement with that of Kinsey and Dumas [2]. To validate the in-house code in solving fluid-structure interaction problems, figure 3 shows that the displacement of the tail compares well with the experiment data for a torsional flexibility model of Toomey and Eldredge[8].

Results

Optimal Kinematic Parameters

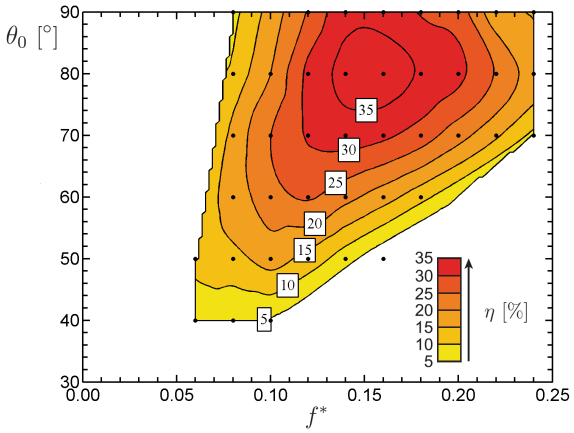

Figure 4: Contours of efficiency of a rigid NACA0015 foil with a rigid flat plate tail at $h_0 = 1$, $\varphi = 90°$ and $x_{piv} = 0.333$

Since a large number of parameters may impact the performance of a flapping foil power generator[11], to reduce the influences of parameters other than flexibility as much as possible, optimal values of kinematic parameters of the rigid case are identified preliminarily from the data in the literature [2] and LBM simulations. In this study, $h_0 = 1$, $\varphi = 90°$ and $x_{piv} =$

0.333 are optimal values suggested by Kinsey and Dumas[2]. The peak efficiency (37.3%) of a rigid foil with a rigid flat plate tail obtained from interpolation of contours generated by LBM simulations in figure 4 corresponds to the operating condition of $f^* = 0.16$ and $\theta_0 = 80^\circ$.

Effects of flexibility

The flexibility is represented by the stiffness k_s. The length $l_{tail} = 0.3c$ and linear density $\rho_{tail} = 10\rho$ of the tail are constants. For comparison with the oscillation frequency of the flapping foil f^*, the flexibility property of the tail is described by a non-dimensional natural frequency of the tail defined as $f_0^* = f_0 c/U = c\sqrt{k_s/J}/(2\pi U)$.

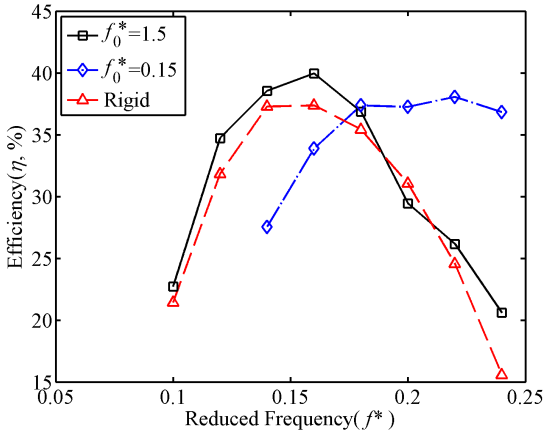

Figure 5: Comparison of the efficiency of a rigid foil with a flexible or a rigid tail at $\theta_0 = 80^\circ$, $h_0 = 1$, $\varphi = 90^\circ$ and $x_{piv} = 0.333$

Power extraction efficiency of a rigid foil with a flexible tail ($f_0^* = 1.5$ and $f_0^* = 0.15$) is compared with the rigid case in a range of $f^* = 0.1 - 0.24$ with constant $\theta_0 = 80^\circ$. In figure 5, the rigid foil with a flexible tail of $f_0^* = 1.5$ shows up to a maximum of 7.24% performance improvement in this range except at $f^* = 0.2$ compared with its rigid counterpart. The peak efficiencies of the rigid foil with a flexible tail of $f_0^* = 1.5$ and with a rigid tail at $f^* = 0.16$ are 40.0% and 37.3% respectively. The efficiency of a rigid foil with a flexible tail of $f_0^* = 0.15$ is only 33.9% at $f^* = 0.16$, whereas within a range of high reduced frequencies ($f^* = 0.18 - 0.24$), the efficiency of the very flexible case is the highest among these three cases. These results indicate that a flexible tail with appropriate frequency ratio ($r = f_0^*/f^* = 9.375$) could enhance the peak efficiency; in addition, according to the definition of the reduced frequency ($f^* = fc/U$), a very flexible tail ($r = 0.9375$) could potentially improve the performance of a flapping foil power generator in low inflow velocity compared to a rigid tail at the same flapping frequency.

Since the highest efficiency of the rigid and flexible tail (40.0%) is achieved at the optimal condition of the rigid case, the influence of the tail flexibility under this condition is further investigated. The instantaneous lift coefficient C_L, angle of tail deflection α_P, power coefficient due to plunge motion C_{Ph}, power coefficient due to pitch motion $C_{P\theta}$ and total power coefficient C_P at the optimal condition ($f^* = 0.16$, $h_0 = 1$, $\theta_0 = 80^\circ$, $\varphi = 90^\circ$ and $x_{piv} = 0.333$)are plotted in figure 6 - figure 8. Since the lift force and prescribed plunge velocity contribute significantly to the power extraction performance[2], the time history of C_L is examined first. As shown in figure 6, the flexible tail of $f_0^* = 1.5$ achieves higher C_L during the middle of the stroke ($t/T = 0.05$-

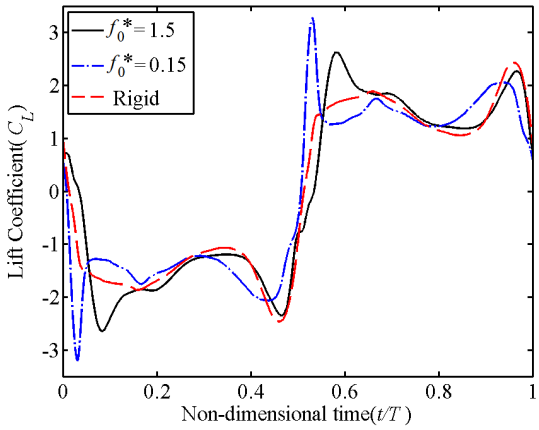

Figure 6: Comparison of the lift coefficient of a rigid foil with a flexible or a rigid tail at $f^* = 0.16$, $\theta_0 = 80^\circ$, $h_0 = 1$, $\varphi = 90^\circ$ and $x_{piv} = 0.333$

0.4 and 0.55-0.8) compared to the rigid one. In addition, the peaks of C_L for flexible tail of $f_0^* = 0.15$ appears earlier than the other two cases, resulting in poor synchronization between lift and plunge motion. These can be partially explained as the position of the tail affects the formation and the trajectory of the trailing edge vortex (TEV), thus affecting the pressure distribution around the foil, especially near the tail.

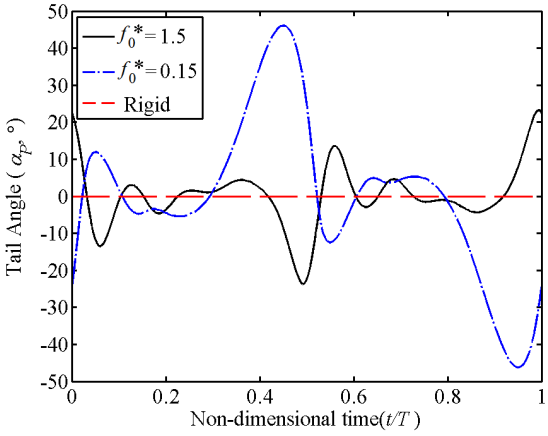

Figure 7: Comparison on the tail angle of a rigid foil with a flexible or a rigid tail at $f^* = 0.16$, $\theta_0 = 80^\circ$, $h_0 = 1$, $\varphi = 90^\circ$ and $x_{piv} = 0.333$

As expected, the peak angle of tail deflection for $f_0^* = 0.15$ is nearly doubled compared to that for $f_0^* = 1.5$ since the former is more flexible (figure 7). In addition, the tail deflection for $f_0^* = 1.5$ and $f_0^* = 0.15$ are in the opposite directions most of the time during the flapping cycle.

Time histories of power coefficients show that C_{Ph} is positive during most of a flapping cycle and its contribution to C_P dominates that of $C_{P\theta}$ (figure 8). During the middle of the stroke, higher C_{Ph} for the flexible tail with $f_0^* = 1.5$ compared to the other two cases can be attributed to the higher C_L shown in figure 6. However, even though near the end of the stroke ($t/T = 0.5$), C_L for $f_0^* = 0.15$ is higher than the other two cases, the low plunge velocity results in low C_{Ph}. In figure 8, a sharp drop in C_P can be observed only for the flexible tail of $f_0^* = 0.15$ near the end of the stroke, while $C_{P\theta}$ for the rigid and flexible

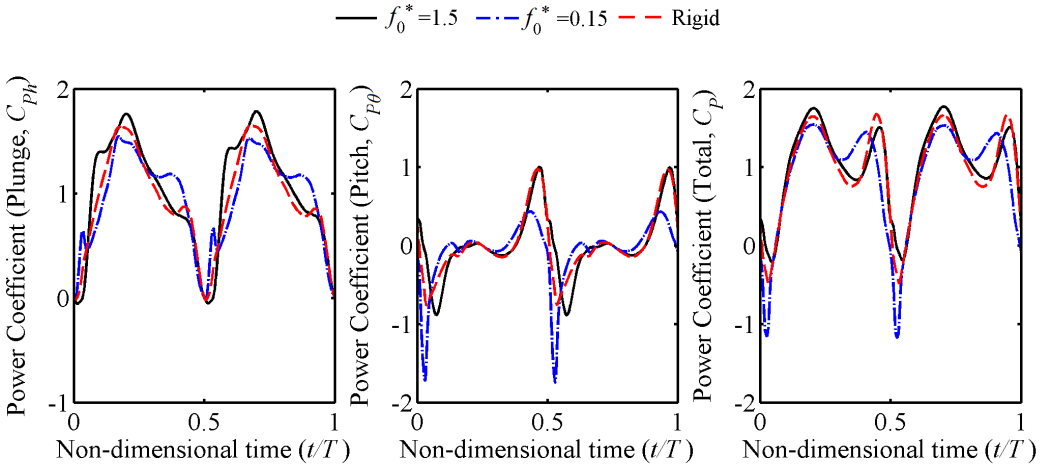

Figure 8: Comparison of the power coefficients of a rigid foil with a flexible or a rigid tail at $f^* = 0.16$, $\theta_0 = 80°$, $h_0 = 1$, $\varphi = 90°$ and $x_{piv} = 0.333$

tail of $f_0^* = 1.5$ is similar with high peak values.

Conclusions

In this study, the influence of flexibility on the performance of a flapping foil power generator is investigated. The model consists of a NACA0015 foil undergoing prescribed pitch and plunge motions and a flat plate tail whose flexibility is modelled by a spring attached to the trailing edge of the foil. An in-house code using the lattice Boltzmann method and immersed boundary method is used to predict the performance and aerodynamic loads.

Results show that the efficiency of a flapping foil power generator can be improved by using a flexible tail with appropriate natural frequency in the range of optimal $f^* = 0.12$-0.18 suggested by parametric studies on rigid foil [11]. Further more, a flexible tail with frequency ratio approaching 10 ($r = 9.375$) enhances the maximum efficiency of a flapping power generator by 7.24% compared to a rigid tail, whereas a more flexible tail ($r = 0.9375$) results in performance reduction under the same condition. However, for f^* in the range 0.2-0.24, the efficiency for the more flexible tail (r=0.9375) is approximately constant at 35% whereas the efficiency for the less flexible tail (r=9.375) and the rigid tail drops sharply from approximately 30% at f^*=0.2 to 20% at f^*=0.24. Detailed examination of the time histories of the lift coefficient and power coefficient show that the flexibility of the tail influences the formation of the LEV and TEV and their interactions, hence the pressure distributions and the performance, especially near the stoke reversal.

Acknowledgements

The author wishes to gratefully acknowledge the receipt of the University International Postgraduate Award (UIPA). This research was undertaken with the assistance of resources from the National Computational Infrastructure (NCI), which is supported by the Australian Government.

References

[1] Hoke, C., Young, J. and Lai, J., Effects of time-varying camber deformation on flapping foil propulsion and power extraction, *Journal of Fluids and Structures*, **56**, 2015, 152–176.

[2] Kinsey, T. and Dumas, G., Parametric study of an oscillating airfoil in a power-extraction regime, *AIAA journal*, **46**, 2008, 1318–1330.

[3] Le, T. Q. and Ko, J. H., Effect of hydrofoil flexibility on the power extraction of a flapping tidal generator via two- and three-dimensional flow simulations, *Renewable Energy*, **80**, 2015, 275–285.

[4] Liu, W., Xiao, Q. and Cheng, F., A bio-inspired study on tidal energy extraction with flexible flapping wings, *Bioinspiration & biomimetics*, **8**, 2013, 036011.

[5] Shoele, K. and Zhu, Q., Performance of a wing with nonuniform flexibility in hovering flight, *Physics of Fluids (1994-present)*, **25**, 2013, 041901.

[6] Tian, F.-B., Luo, H., Zhu, L., Liao, J. C. and Lu, X.-Y., An efficient immersed boundary-lattice boltzmann method for the hydrodynamic interaction of elastic filaments, *Journal of computational physics*, **230**, 2011, 7266–7283.

[7] Tian, F.-B., Young, J. and Lai, J. C., Improving power-extraction efficiency of a flapping plate: From passive deformation to active control, *Journal of Fluids and Structures*, **51**, 2014, 384–392.

[8] Toomey, J. and Eldredge, J. D., Numerical and experimental study of the fluid dynamics of a flapping wing with low order flexibility, *Physics of Fluids (1994-present)*, **20**, 2008, 073603.

[9] Wu, J., Shu, C., Zhao, N. and Tian, F.-B., Numerical study on the power extraction performance of a flapping foil with a flexible tail, *Physics of Fluids (1994-present)*, **27**, 2015, 013602.

[10] Xiao, Q. and Zhu, Q., A review on flow energy harvesters based on flapping foils, *Journal of Fluids and Structures*, **46**, 2014, 174–191.

[11] Young, J., Lai, J. C. and Platzer, M. F., A review of progress and challenges in flapping foil power generation, *Progress in Aerospace Sciences*, **67**, 2014, 2–28.